Available online at www.sciencedirect.com

SciVerse ScienceDirect

Ceramics International 38 (2012) 5103–5112

CERAMICS INTERNATIONAL

www.elsevier.com/locate/ceramint

Approaches for preparing ⟨1 1 1⟩-textured $Bi_{0.5}Na_{0.5}TiO_3$-based ceramics by hetero-templated grain growth

Yuka Negishi, Toshio Kimura *

Graduate School of Science and Technology, Keio University, 3-14-1 Hiyoshi, Kohoku-ku, Yokohama 223-8522, Japan

Received 16 February 2012; accepted 4 March 2012
Available online 12 March 2012

Abstract

The preparation of ⟨1 1 1⟩-textured $Bi_{0.5}Na_{0.5}TiO_3$ (BNT) ceramics was attempted by the templated grain growth method. This method uses anisometric grains as the template for texture development. In this work, plate-like $BaTiO_3$ grains with the ⟨1 1 1⟩ direction perpendicular to the plate faces were used. A mixture of the plate-like $BaTiO_3$ grains and equiaxed BNT grains was consolidated by tape casting to prepare green compacts in which the plate-like $BaTiO_3$ grains were dispersed in the matrix of the BNT grains and were aligned with their plate faces parallel to the casting direction. The textured BNT ceramics could not be obtained by the sintering of the green compacts, because of the disappearance of the plate-like $BaTiO_3$ grains by dissolution in the BNT grains. Several approaches were examined to obtain ⟨1 1 1⟩-textured ceramics. They included the use of plate-like (Sr, Ba)TiO_3 grains as the template, the use of equiaxed grains of BNT–$BaTiO_3$ and BNT–$Bi_{0.5}K_{0.5}TiO_3$ solid solutions as the matrix, and the addition of excess Na_2CO_3 and Bi_2O_3 to form liquid phases. The only approach successful in obtaining the textured ceramics was the one involving the addition of excess Na_2CO_3. The excess Na_2CO_3 formed a liquid phase and promoted the formation of a shell of BNT grains around a plate-like $BaTiO_3$ grain, prior to the dissolution of the $BaTiO_3$ grain. The BNT shell had the same crystallographic orientation as the $BaTiO_3$ grain and acted as the template for texture development.

Keywords: Texture development; Microstructure development; Templated grain growth; Bismuth sodium titanate; Barium titanate

1. Introduction

Texture engineering is an important technique for enhancing the properties of ceramics [1]. An increase in the piezoelectric constant by 50–100% has been reported in various systems [1,2]. Textured ceramics can be obtained by various methods and templated grain growth (TGG) is one of the most convenient ones. In this method, anisometric and equiaxed grains with the same composition are used [2]. A green compact consisting of aligned anisometric grains in a matrix of equiaxed grains is sintered. Highly textured ceramics are obtained by the growth of the anisometric grains at the expense of the equiaxed grains [3,4] or by the morphological change of the equiaxed grains in the presence of the anisometric grains [5,6]. In both cases, the anisometric grains act as templates for the texture development. Therefore, the anisometric and equiaxed grains are called template and matrix grains, respectively. When the anisometric grains are not available, the reactive-templated grain growth method is employed [7,8]. In this method, the template grains are formed by the in situ reaction of anisometric precursor grains (reactive template grains) with complementary materials during the calcination of the green compact. When both the template and reactive template grains are not available, hetero-template grains are employed [1,9,10], i.e., template grains with a composition different from that of the matrix grains are used. For example, $Pb(Mg_{1/3}Nb_{2/3})O_3$–$PbTiO_3$ is textured by plate-like $BaTiO_3$ and $SrTiO_3$ grains [9].

Plate-like grains with the perovskite structure are used in many cases, because materials with the perovskite structure have excellent piezoelectric properties. Although the piezoelectric phase of perovskite materials can have a tetragonal, rhombohedral, or orthorhombic structure, the anisotropy in their crystallographic properties is small. Because the grain shape is determined by the relative growth rate of each crystallographic plane, the anisometric grains are difficult to obtain by simple preparation from raw materials such as $BaCO_3$

---

* Corresponding author. Tel.: +81 45 566 1565; fax: +81 45 566 1551.
E-mail address: kimura@applc.keio.ac.jp (T. Kimura).

0272-8842/$36.00 © 2012 Elsevier Ltd and Techna Group S.r.l. All rights reserved.
doi:10.1016/j.ceramint.2012.03.013

and TiO_2. Plate-like perovskite grains are obtained from precursor materials with layered perovskite structures such as the Ruddlesden-Popper and Aurivillius structures [11–18]. These precursors give plate-like perovskite grains with the $\langle 1\,0\,0\rangle$ direction perpendicular to the plate face. Therefore, a $\langle 1\,0\,0\rangle$ texture can be given to the piezoelectric material with the perovskite structure by the homo- and hetero-templated grain growth methods.

In some materials with the perovskite structure, a direction other than $\langle 1\,0\,0\rangle$ gives the highest piezoelectric properties [19]. For these materials, plate-like grains with the $\langle 1\,1\,1\rangle$ and $\langle 1\,1\,0\rangle$ directions perpendicular to the plate face are necessary to obtain $\langle 1\,1\,1\rangle$- and $\langle 1\,1\,0\rangle$-textured materials. However, the grains available so far have been limited to those of $BaTiO_3$ [20,21]. Materials other than $BaTiO_3$ must be textured by the hetero-templated grain growth method using $BaTiO_3$ template grains. However, it has been reported that plate-like $BaTiO_3$ grains are unstable in the preparation of $\langle 1\,0\,0\rangle$-textured $Bi_{0.5}Na_{0.5}TiO_3$-$BaTiO_3$, and plate-like $SrTiO_3$ grains are used as hetero-templates [10]. In the present work, we have tried to prepare $\langle 1\,1\,1\rangle$-textured $Bi_{0.5}Na_{0.5}TiO_3$ (BNT). The only candidate suitable for use as the template grain is $BaTiO_3$. First, we have examined the origin of the instability of the plate-like $BaTiO_3$ grains and found that it was due to the dissolution of $BaTiO_3$ in BNT. Further, several approaches were used to prepare textured materials. These included the use of plate-like (Sr, Ba)TiO_3 grains as the template, the use of BNT–$BaTiO_3$ and BNT–$Bi_{0.5}K_{0.5}TiO_3$ (BKT) solid solutions as the matrix, and the formation of a liquid phase by adding excess Na_2CO_3 and Bi_2O_3 [22,23].

2. Experimental procedure

2.1. Chemicals

The powders used in this experiment were the following: $BaTiO_3$ purchased from Sakai Chemical Industry Co., Ltd., Osaka, Japan; TiO_2 from Ishihara Sangyo Kaisha, Ltd., Osaka, Japan; Bi_2O_3 and $SrCO_3$ from Kojundo Chemical Laboratory Co. Ltd., Saitama, Japan; and Na_2CO_3, K_2CO_3, $BaCO_3$, NaCl, and KCl from Wako Pure Chemical Industries Ltd., Osaka, Japan. These were reagent-grade powders. The powders were used without further treatments such as purification. The materials for tape-casting were ethanol (solvent; Amakasu Chemical Industries, Tokyo, Japan), toluene (solvent; Wako Pure Chemical Industries Ltd., Osaka, Japan), poly(vinyl butyral) (binder; S-LEC BH-3, Sekisui Chemical Co., Ltd., Tokyo, Japan), di-*n*-butyl phthalate (plasticizer; Wako Pure Chemical Industries Ltd., Osaka, Japan), and polyoxyethylene alkyl ether phosphoric acid (dispersant; Phosphor Knoll RS-710, Toho Chemical Industry Co., Ltd., Tokyo, Japan).

2.2. Template powders

Powders of plate-like $BaTiO_3$ and (Sr, Ba)TiO_3 was prepared by a two-step process [20]. First, $BaTiO_3$ and TiO_2 in the molar ratio 6:9 (BaO-rich) were mixed with a ball mill to compensate for the loss of Ba in the molten salt [24]. The mixture was dry-mixed with NaCl–KCl (molar ratio of 1:1) in a weight ratio of 1:1, and heated at 820 °C for 1 h to melt the NaCl–KCl in the mixture and then at 1150 °C for 5 h to prepare plate-like $Ba_6Ti_{17}O_{40}$ grains. The product was washed with water many times to remove NaCl–KCl. Then, the obtained $Ba_6Ti_{17}O_{40}$ powder was reacted with $BaCO_3$ or $SrCO_3$ (molar ratio of 1:11) at 1150 °C for 5 h in molten NaCl to obtain plate-like $BaTiO_3$ or (Sr, Ba)TiO_3 grains with (1 1 1) major faces. The product was repeatedly washed with water as in the first step.

2.3. Matrix powders

The matrix powders were prepared by the conventional solid-state reaction method. Stoichiometric mixtures of Bi_2O_3, Na_2CO_3, K_2CO_3, and TiO_2, corresponding to $Bi_{0.5}(Na_{1-x}K_x)_{0.5}TiO_3$ ($x = 0$, 0.3, and 0.5) stoichiometry, were ball-milled for 24 h using ethanol as a medium and calcined at 900 °C for 3 h. The products were ball-milled for 48 h in ethanol with 2 mm ZrO_2 balls. The matrix powders were in a single phase as confirmed by an X-ray diffraction analysis. The grains were equiaxed and irregular in shape, and most of the grains were between 0.3 and 0.5 μm in size, as confirmed with a scanning electron microscope (SEM). The powders with $x = 0$, 0.3, and 0.5 are abbreviated as BNT, BNKT0.3, and BNKT0.5, respectively. The matrix powders containing excess Na_2CO_3 and Bi_2O_3 had a molar ratio of BNT:Na_2CO_3 = 1:0.005 and BNT:Bi_2O_3 = 1:0.005, respectively. Excess Na_2CO_3 and Bi_2O_3 were added to the mixtures for tape casting.

2.4. Sample preparation

Five types of specimens were prepared; the names and compositions of the mixtures are listed in Table 1. The specimens were consolidated by tape casting. The slurries for tape casting were prepared by the following procedure. The template and matrix powders (total 25 g) were mixed in a solvent (60 vol% toluene and 40 vol% ethanol; 23.6 cm^3) containing the dispersant (0.50 cm^3) using a planetary ball-mill for 30 min. Then, the binder and plasticizer (both 1.69 g) were added to the mill and mixed for 90 min. The slurries were tape-cast to form sheets in which the template grains were aligned with their plate face parallel to the sheet surface. The sheets were cut into pieces of size 30 mm × 30 mm, and the pieces were laminated and pressed in a die at 80 °C and 50 MPa for 3 min to form green compacts with a thickness of about 2 mm. The compacts were further cut into small pieces (10 mm × 10 mm). They were heated at 500 °C for 2 h to remove organic substances, and were then sintered under various conditions (the heating rate was 100 °C/h).

2.5. Characterization

The crystalline phases and the degree of orientation were evaluated by X-ray diffraction (XRD) analysis (D8

Table 1
Compositions of sample mixtures.

Sample name	The amount of materials	
	Template	Matrix
$BaTiO_3$–BNT	$BaTiO_3$ (20 wt%)	BNT (80 wt%)
(Sr, Ba)TiO_3–BNT	(Sr, Ba)TiO_3 (20 wt%)	BNT (80 wt%)
$BaTiO_3$–(BNT + $BaTiO_3$)	$BaTiO_3$ (10 wt%)	BNT (80 wt%) + $BaTiO_3$ (10 wt%)
$BaTiO_3$–BNKTx	$BaTiO_3$ (20 wt%)	BNKT-x (80 wt%)
$BaTiO_3$–(BNT + Na_2CO_3)	$BaTiO_3$ (20 wt%)	BNT (79.2 wt%) + Na_2CO_3 (0.8 wt%)
$BaTiO_3$–(BNT + Bi_2O_3)	$BaTiO_3$ (20 wt%)	BNT (79.12 wt%) + Bi_2O_3 (0.88 wt%)

ADVANCE, Bruker AXS, Karlsruhe, Germany) using Cu Kα radiation on the major surface (the same as the sheet surface). The degree of orientation was evaluated from the diffraction lines between $2\theta = 20^\circ$ and 60° by the Lotgering factor (F) [25]. The microstructure was observed using an SEM (XL-30 ESEM, Philips, Eindhoven, The Netherlands). The density of samples was measured by Archimedes' method.

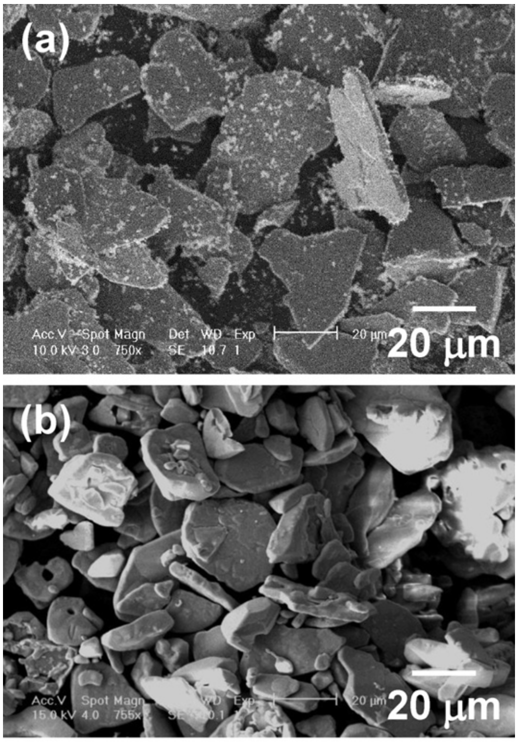

Fig. 1. SEM photographs of (a) $Ba_6Ti_{17}O_{40}$, (b) $BaTiO_3$, and (c) (Sr, Ba)TiO_3 powders.

3. Results and discussion

3.1. Template powders

Fig. 1 shows the SEM micrographs of the intermediate $Ba_6Ti_{17}O_{40}$ powder and the template $BaTiO_3$ and (Sr, Ba)TiO_3 powders. The $Ba_6Ti_{17}O_{40}$ power was mainly composed of large plate-like grains with diameters ranging from 20 to 50 μm and a thickness of 3 μm. The powder contained small impurity grains. This impurity resulted from the difference in the solubilities of BaO and TiO_2 in NaCl–KCl. To compensate for this difference, a Ba-rich composition was employed to prepare $Ba_6Ti_{17}O_{40}$, but the composition of the solid phases deviated from Ba:Ti = 6:17 to some extent, resulting in the formation of the impurity. The composition of this impurity might be $BaTiO_3$ (Ba-poor) or $Ba_4Ti_{13}O_{30}$ (Ba-rich), based on the phase diagram of the $BaTiO_3$–TiO_2 system [26].

Fig. 2 shows the XRD patterns of the reaction products (template grains) of $Ba_6Ti_{17}O_{40}$ with $BaCO_3$ and $SrCO_3$. All the diffraction lines were assigned to the perovskite structure. This indicates the formation of $BaTiO_3$ and $Ba_{0.353}Sr_{0.647}TiO_3$. The $BaTiO_3$ powder (Fig. 1(b)) was composed of plate-like grains with diameters ranging from 10 to 30 μm and thicknesses of 3–4 μm. The diameter had reduced and the thickness had increased a little. The most intense diffraction line was changed from {1 1 0}, which is the most intense line for randomly oriented $BaTiO_3$ grains, to {1 1 1} by the preferred orientation of plate-like grains. This indicated that the ⟨1 1 1⟩ direction was perpendicular to the plate face. In the $Ba_{0.353}Sr_{0.647}TiO_3$ powder (Fig. 1(c)), a small number of plate-like grains with shapes and sizes similar to those of the plate-like $BaTiO_3$ grains were present, but many of the grains had disintegrated into little pieces with small aspect ratios.

3.2. Instability of $BaTiO_3$ in $Bi_{0.5}Na_{0.5}TiO_3$ (BNT)

The green compacts of $BaTiO_3$–BNT (see Table 1 for the composition of the specimen) were heated at various temperatures between 950 °C and 1200 °C for 2 h. Fig. 3 shows the XRD patterns of the sintered compacts. The diffraction pattern of the matrix BNT powder is also shown for comparison. The diffraction lines of BNT and $BaTiO_3$ were confirmed in the specimen heated at 950 °C. The most intense lines of BNT and $BaTiO_3$ were {1 1 0} and {1 1 1}, respectively, indicating that the plate-like $BaTiO_3$ grains were oriented with their plate faces parallel to the specimen surface,

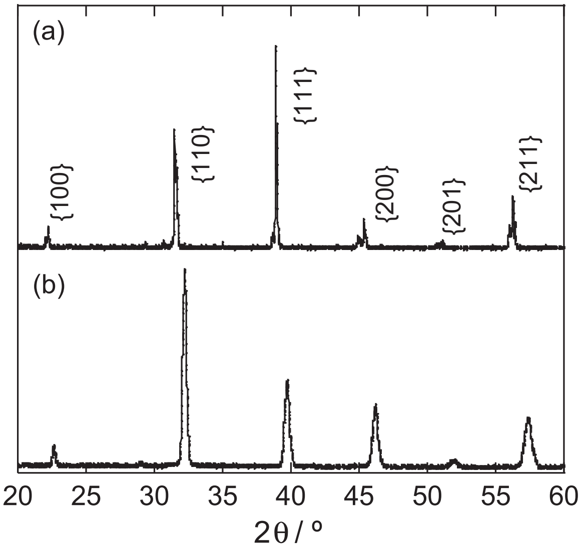

Fig. 2. XRD patterns of reaction products (template grains) of $Ba_6Ti_{17}O_{40}$ with (a) $BaCO_3$ and (b) $SrCO_3$.

because {1 1 0} is the most intense line for randomly oriented BNT and $BaTiO_3$ grains. The relative intensity of the diffraction lines belonging to $BaTiO_3$ decreased with an increase in heating temperature, and finally, it became zero in the specimen heated at 1150 °C. At the same time, the diffraction lines belonging to BNT moved towards the lower angles and the {2 0 0} line split into two lines. Fig. 4 shows the microstructures of the specimens heated at 1050 °C, 1100 °C, and 1200 °C for 2 h. Cross sections of the plate-like $BaTiO_3$ grains were confirmed in the specimen heated at 1050 °C, but these grains were not observed in the specimens heated at 1100 °C and 1200 °C. Instead, these specimens contained many elongated pores.

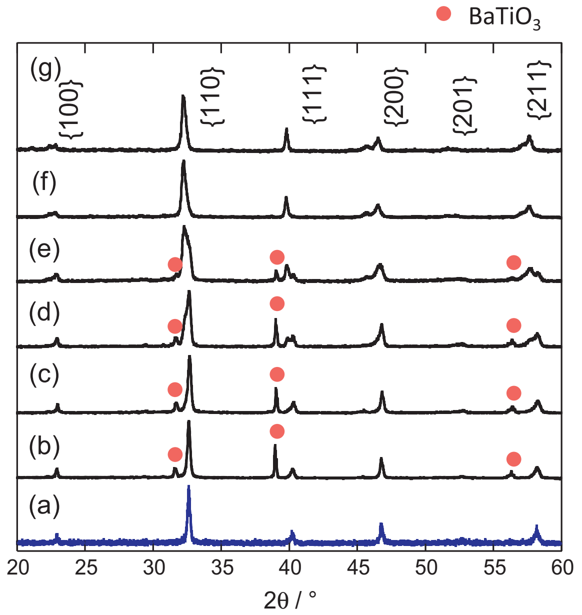

Fig. 3. XRD patterns of (a) BNT powder and $BaTiO_3$–BNT sintered for 2 h at (b) 950 °C, (c) 1000 °C, (d) 1050 °C, (e) 1100 °C, (f) 1150 °C, and (g) 1200 °C.

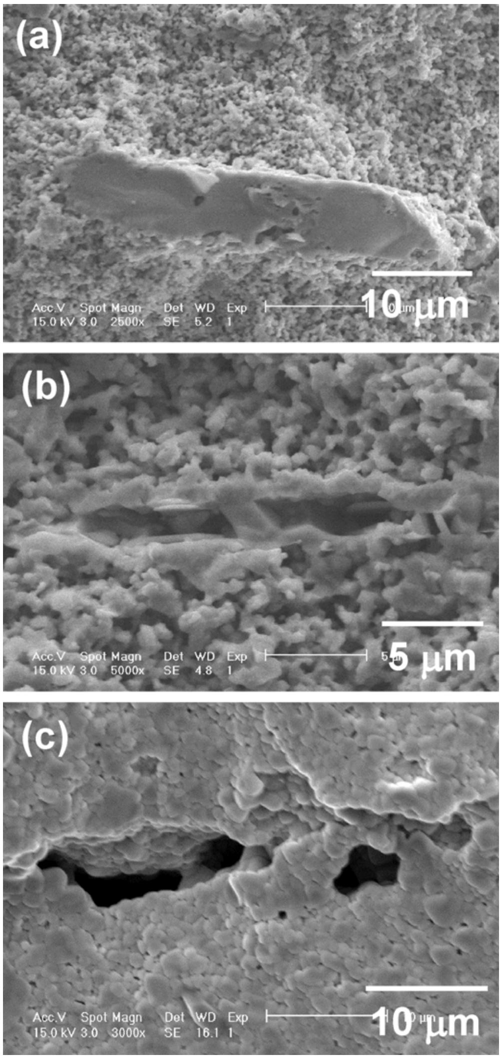

Fig. 4. Microstructures of $BaTiO_3$–BNT sintered at (a) 1050 °C, (b) 1100 °C, and (c) 1200 °C for 2 h.

The presence of the elongated pores and the disappearance of the diffraction lines of $BaTiO_3$ suggest that the cause of the instability of the $BaTiO_3$ grains in BNT is the dissolution of $BaTiO_3$ in BNT. The dissolution of template grains in the matrix phase has been reported for several systems [27,28]. The formation of the elongated pores indicates that $BaTiO_3$ dissolves in BNT by the one-dimensional diffusion of $BaTiO_3$. The composition of the matrix phase changes from pure BNT to a BNT–$BaTiO_3$ solid solution. If a homogeneous solid solution forms, the composition is $(Bi_{0.5}Na_{0.5})_{0.815}Ba_{0.185}TiO_3$. The crystal structure changes from orthorhombic with a small α value (89.83°) [29] to tetragonal (the morphotropic phase boundary lies at 6–7 mol% $BaTiO_3$ [30]). The dissolution of $BaTiO_3$ in BNT increases the lattice parameters and the splitting of $\{2\,0\,0\}_{ortho}$ into $\{2\,0\,0\}_{tetra}$ and $\{0\,0\,2\}_{tetra}$; these are observed in Fig. 3.

Several approaches were used to overcome the instability of the $BaTiO_3$ templates. The first involved using plate-like (Sr, Ba)TiO_3 grains as templates to reduce the chemical potential of $BaTiO_3$ in the template grains. Furthermore, $SrTiO_3$ does not dissolve in BNT [10]. The second approach involved using BNT–$BaTiO_3$ solid solutions as the matrix to increase the chemical potential of $BaTiO_3$ in the matrix phase. In the third approach, $Bi_{0.5}(Na_{1-x}K_x)_{0.5}TiO_3$ (BNKT-x) was used as the matrix to reduce the diffusion rate of $BaTiO_3$ in the matrix phase. The substitution of K ions for Na ions changes the grain boundary structure at an atomic scale from rough to smooth [31], and the diffusion rate is expected to be reduced along atomically smooth grain boundaries [32]. The fourth approach involved using a liquid phase to promote the formation of oriented regions around the $BaTiO_3$ templates before the disappearance of $BaTiO_3$ [22,23].

3.3. Approaches to prepare textured ceramics

3.3.1. Use of (Sr, Ba)TiO_3 templates

The compacts of (Sr, Ba)TiO_3–BNT (see Table 1 for the composition of the specimen) were heated at 1000 °C, 1100 °C, and 1200 °C for 2 h. Figs. 5 and 6 show the XRD patterns and microstructures of the specimens, respectively. The relative intensity of {1 1 1} did not increase, and the (Sr, Ba)TiO_3 peaks shifted to the high-diffraction-angle side. The microstructure at 1000 °C was composed of dense grains and a porous matrix. The dense grains were elongated in shape, and their longer axis was aligned parallel to the major surface of the specimen. These grains were derived from the (Sr, Ba)TiO_3 templates. The size of the grains derived from the templates increased at 1100 °C, but these grains could not be distinguished from grains grown from the matrix grains in the specimen sintered at 1200 °C. In the specimen sintered at 1200 °C, no elongated pores were present and large grains with facets were confirmed among the irregularly shaped grains.

Fig. 7 shows the distribution of elements in the specimen sintered at 1200 °C for 2 h. A region with high concentration of Sr was detected in the center of the faceted grain. The concentration of Ba was also high in the same region. Ba was also detected in the outer part of the grain. Bi was distributed in all the parts except for the regions with a high concentration of Sr. The distribution of the elements indicates that the faceted grain develops from the template grains, i.e., the center is the template (Sr, Ba)TiO_3 grain and the outer part is derived from the matrix BNT grains. The Ba in the (Sr, Ba)TiO_3 grain diffuses into BNT but Sr does not. Bi (and also Na) does not diffuse into (Sr, Ba)TiO_3.

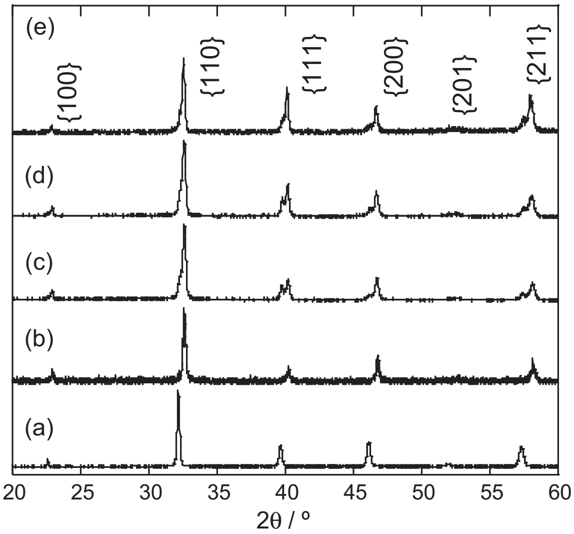

Fig. 5. XRD patterns of (a) (Sr, Ba)TiO_3 and (b) BNT powders and (Sr, Ba)TiO_3–BNT sintered for 2 h at (c) 1000 °C, (d) 1100 °C, and (e) 1200 °C.

The (Sr, Ba)TiO_3 grains act as a template for the grain growth of BNT, forming grains with the core of (Sr, Ba)TiO_3 and the shell of BNT–$BaTiO_3$. It is reported that grains with a

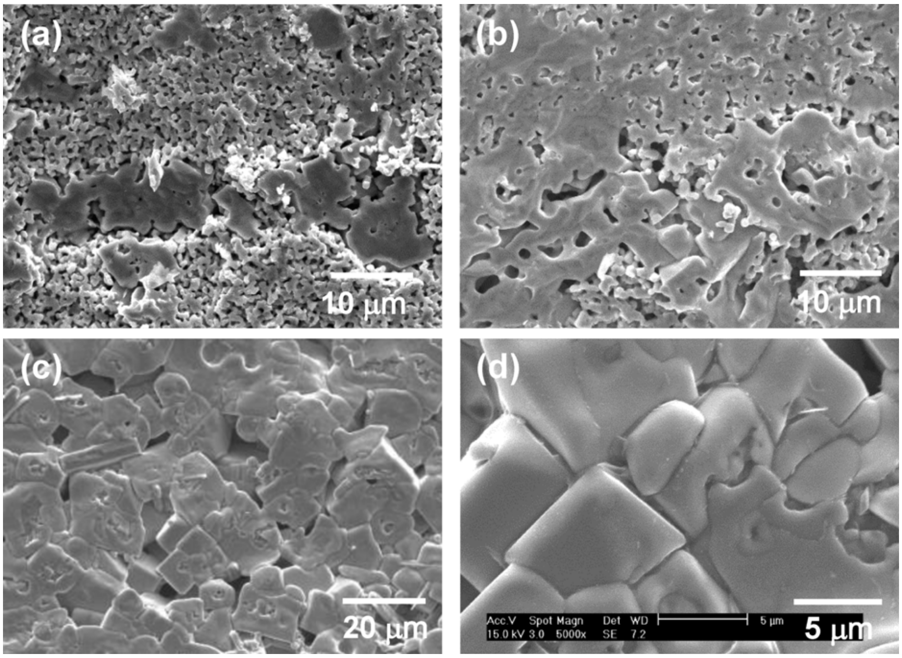

Fig. 6. Microstructures of (Sr, Ba)TiO_3–BNT sintered at (a) 1000 °C, (b) 1100 °C, and (c and d) 1200 °C for 2 h.

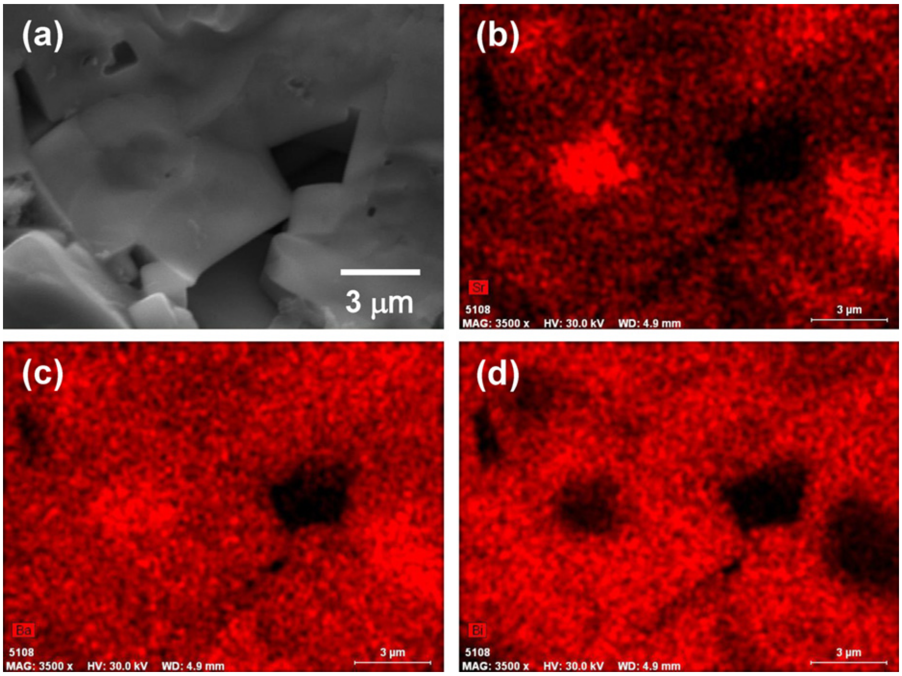

Fig. 7. Distribution of (b) Sr, (c) Ba, and (d) Bi in (Sr, Ba)TiO_3–BNT sintered at 1200 °C for 2 h. The SEM image of measured area is shown in (a).

cubic shape develop in BNT–$BaTiO_3$ [33], and the crystallographic planes of the facets are {1 0 0}. The angle between the {1 0 0} planes and the major surface of the specimen is about 45°, indication that the ⟨1 1 1⟩ direction is perpendicular to the major surface of the specimen. Therefore, it is evident that the (Sr, Ba)TiO_3 grains act as templates for texture development. However, the degree of orientation for the specimen sintered at 1200 °C was very low (0.15), and is caused by the shape of (Sr, Ba)TiO_3 grains (Fig. 1(c)). A major portion of the (Sr, Ba)TiO_3 grains are small with low aspect ratios. Therefore, it is not expected that these grains have an orientation in which their plate face is parallel to the casting direction. Although large plate-like grains align with their plate face parallel to the casting direction as shown in Fig. 6(a), the number of these grains is small, resulting in a low degree of orientation. It can be concluded that the (Sr, Ba)TiO_3 grains acted as the template for ⟨1 1 1⟩ texture formation, but the disintegration of the grains into smaller pieces during the conversion from $Ba_6Ti_{17}O_{40}$ to (Sr, Ba)TiO_3 reduces the grain size and also broadens the orientation direction of plate-like grains.

3.3.2. Use of BNT–$BaTiO_3$ matrix

The driving force for the dissolution of the template $BaTiO_3$ grains is caused by the difference in the chemical potential of $BaTiO_3$ between the template and matrix grains. When $BaTiO_3$ powder with a small size is added to the BNT matrix, it is expected that fine $BaTiO_3$ grains dissolve in the BNT matrix, prior to the dissolution of the template $BaTiO_3$ grains, and increase the chemical potential of $BaTiO_3$ in the matrix grains. Accordingly, the $BaTiO_3$–(BNT + $BaTiO_3$) specimen was examined (see Table 1 for the composition of the specimen). The overall composition was the same as that of $BaTiO_3$–BNT. The green compacts were heated at various temperatures for 2 h. The result was the same as that for $BaTiO_3$–BNT. The XRD lines of $BaTiO_3$ disappeared at 1100 °C and elongated pores were formed in the compacts heated at and above 1100 °C. These results indicate that the addition of fine $BaTiO_3$ grains to the matrix phase does not retard the dissolution of plate-like $BaTiO_3$ grains.

3.3.3. Use of BNKT matrix

Equiaxed grains of BNKT0.3 and BNKT0.5 were used as the matrix grains. Fig. 8 shows the XRD patterns of the specimen heated at various temperatures for 2 h. The diffraction lines of $BaTiO_3$ disappeared in the specimens sintered at 1150 °C and 1100 °C for BNKT0.3 and BNKT0.5, respectively. The elongated pores were also observed in these specimens. A comparison of Fig. 8 with Fig. 3 illustrates the effect of the chemical composition of the matrix phase on the rate of dissolution of $BaTiO_3$. The {1 1 1} line of $BaTiO_3$ was confirmed in the $BaTiO_3$–BNT and $BaTiO_3$–BNKT0.3 specimens sintered at 1100 °C, but the relative intensity of the {1 1 1} line of $BaTiO_3$ was higher than that of the {1 1 1} line of BNKT in the $BaTiO_3$–BNKT0.3 specimen, whereas in the $BaTiO_3$–BNT specimen, it was vice versa. This result indicates that the dissolution of the $BaTiO_3$ grains was retarded by using the BNKT0.3 matrix. On the other hand, in the $BaTiO_3$–BNKT0.5 specimen, the diffraction lines of $BaTiO_3$ disappeared in the specimen sintered at 1100 °C, indicating that the BNKT0.5 matrix promoted the dissolution of $BaTiO_3$.

The effectiveness of plate-like $BaTiO_3$ grains in the formation of texture is evaluated for the specimens heated at 1200 °C. The $BaTiO_3$–BNKT0.3 specimen has the highest F value (0.21), followed by BNT (0.11) and $BaTiO_3$–BNKT0.5 (0.03).

These data indicate that the substitution of K ions for Na ions retards the dissolution of plate-like $BaTiO_3$ grains but excessive

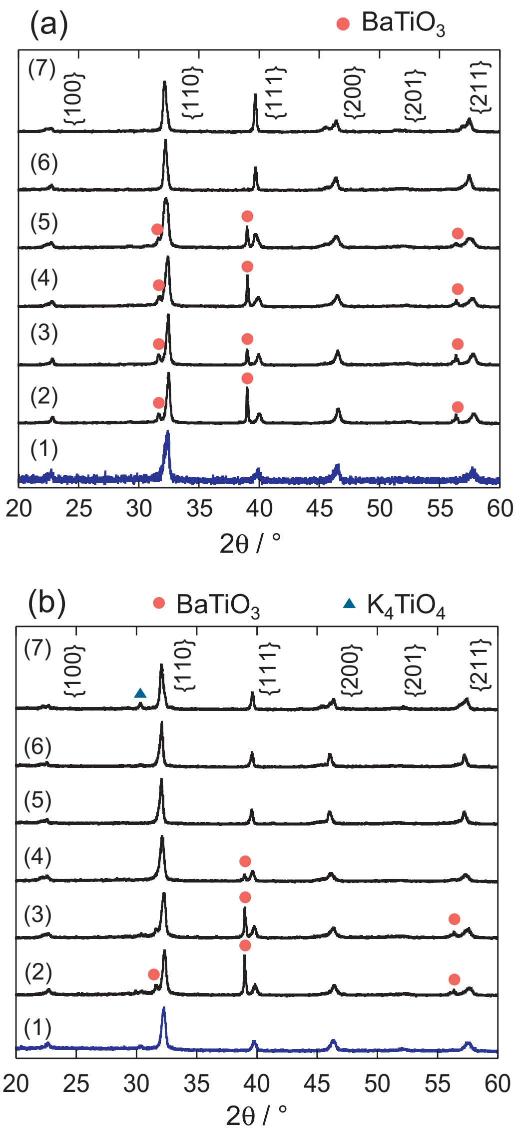

Fig. 8. XRD patterns of (a) $BaTiO_3$–BNKT0.3 and (b) $BaTiO_3$–BNKT0.5 sintered for 2 h at (2) 950 °C, (3) 1000 °C, (4) 1050 °C, (5) 1100 °C, (6) 1150 °C, and (7) 1200 °C. XRD patterns of BNKT0.3 and BNKT0.5 are shown in (a)(1) and (b)(1), respectively.

substitution results in the promotion of the dissolution. The structure of the grain boundaries is atomically rough in BNT. The substitution of K ions for Na ions makes the structure atomically smooth [31] and the diffusion rate of $BaTiO_3$ in the matrix phase is reduced. However, this reduction is not enough to prevent the dissolution of the template $BaTiO_3$ grains. Further substitution ($x = 0.5$) of the large K ions increases the lattice parameter, promotes the diffusion of Ba ions in the BNKT grains, and cancels the effect of the grain boundary structure on the diffusion.

3.3.4. *Use of liquid phase*

Fig. 9 shows the XRD patterns of the $BaTiO_3$–(BNT + Na_2CO_3) specimens containing excess Na_2CO_3 (see Table 1 for the composition) heated at various temperatures for 2 h. The diffraction lines belonging to $BaTiO_3$ disappeared in the specimens heated at and above 1100 °C. The temperature at which $BaTiO_3$ disappeared was lower than that for $BaTiO_3$–BNT (Fig. 3). However, $\{1\,1\,1\}$ was the most intense line in the specimen heated at 1200 °C, indicating that $\langle 1\,1\,1 \rangle$ texture developed in spite of the disappearance of the $BaTiO_3$ template grains. The degree of orientation was 0.37.

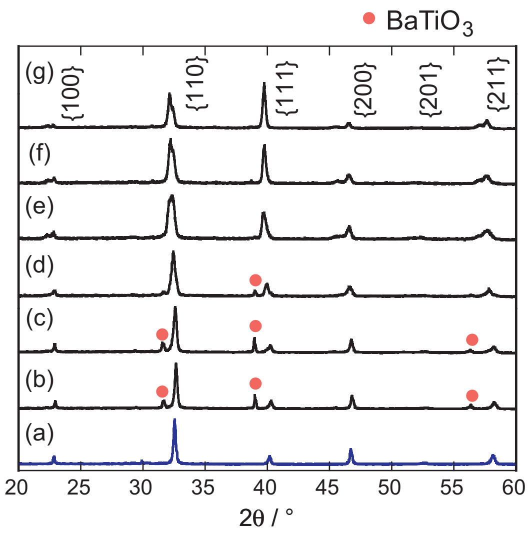

Fig. 9. XRD patterns of (a) BNT + Na_2CO_3 powder and $BaTiO_3$–(BNT + Na_2CO_3) sintered for 2 h at (b) 950 °C, (c) 1000 °C, (d) 1050 °C, (e) 1100 °C, (f) 1150 °C, and (g) 1200 °C.

Fig. 10 shows the microstructures of the $BaTiO_3$–(BNT + Na_2CO_3) specimens sintered at various temperatures for 2 h. The microstructure of the specimen sintered at 1000 °C was the same as that of $BaTiO_3$–BNT sintered at 1050 °C (Fig. 4(a)). In the specimens sintered at 1050 °C, layers of matrix grains formed on the surface of template grains, and these layers thickened and surrounded the plate-like $BaTiO_3$ grains in the specimen heated at 1100 °C. These grains are called template BNT grains. The size of the template BNT grains increased with an increase in the sintering temperature. In the specimen sintered at and above 1150 °C, the plate-like $BaTiO_3$ grains disappeared and large pores were formed in the template BNT grains as shown in Fig. 10(c) and (d). In spite of the disappearance of the plate-like $BaTiO_3$ grains, the $\langle 1\,1\,1 \rangle$-texture developed, for which the growth of the template BNT grains at the expense of the matrix BNT grains was responsible.

Fig. 11 shows the XRD patterns of the $BaTiO_3$–(BNT + Bi_2O_3) specimens sintered at various temperatures for 2 h (see Table 1 for the composition). The diffraction lines belonging to $BaTiO_3$ disappeared in the specimens heated at and above 1100 °C. The intensity of $\{1\,1\,1\}$ did not increase with an increase in heating temperature, unlike in the case of the $BaTiO_3$–(BNT + Na_2CO_3) specimen. Fig. 12 shows the microstructures of the $BaTiO_3$–(BNT + Bi_2O_3) specimens. In the specimen sintered at 1050 °C, the plate-like $BaTiO_3$ grains were present but no dense region developed around the $BaTiO_3$ grains. At 1100 °C, the plate-like $BaTiO_3$ grains disappeared (Fig. 12(b)).

Both excess Na_2CO_3 and Bi_2O_3 form liquid phases [22,23], but their individual effect on the microstructure development is

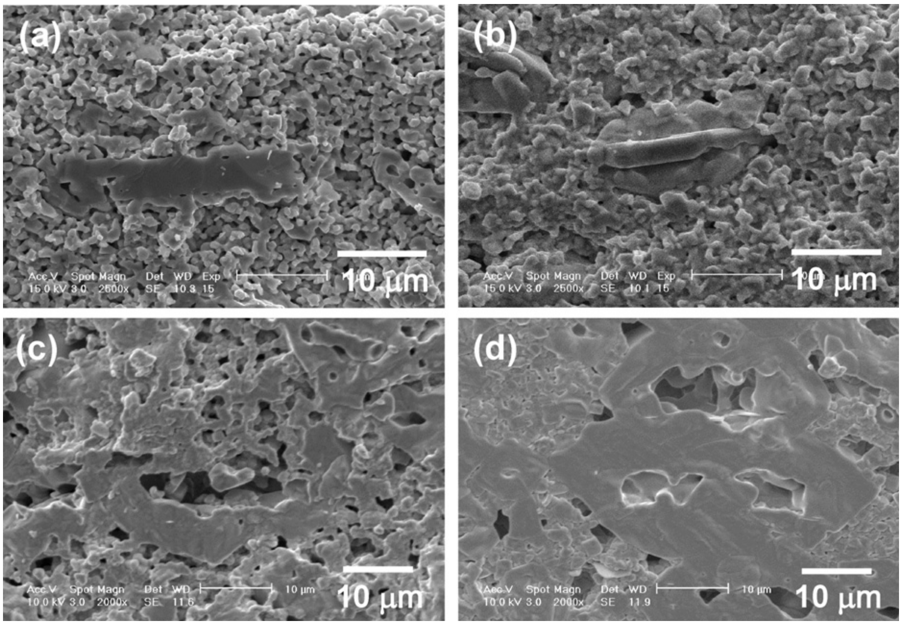

Fig. 10. Microstructures of $BaTiO_3$–(BNT + Na_2CO_3) sintered at (a) 1050 °C, (b) 1100 °C, and (c) 1150 °C, and (d) 1200 °C for 2 h.

different. Fig. 13 shows the densification behavior of the $BaTiO_3$–BNT, $BaTiO_3$–(BNT + Na_2CO_3), and $BaTiO_3$–(BNT + Bi_2O_3) specimens. Excess Bi_2O_3 promoted densification but excess Na_2CO_3 did not. The comparison of the microstructure of the specimens with and without excess Na_2CO_3 heated at 1050 °C (Fig. 4(a) and Fig. 10(a)) indicates that excess Na_2CO_3 promotes grain growth. In the specimen containing excess Na_2CO_3, the BNT grains adjacent to the plate-like $BaTiO_3$ grains grow to form the template BNT grains. The template BNT grains have the same crystallographic orientation as the plate-like $BaTiO_3$ grains.

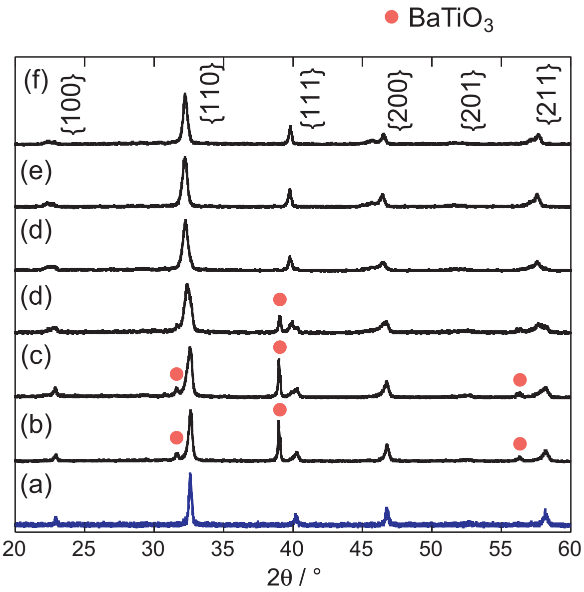

Fig. 11. XRD patterns of (a) BNT + Bi_2O_3 powder and $BaTiO_3$–(BNT + Bi_2O_3) sintered for 2 h at (b) 950 °C, (c) 1000 °C, (d) 1050 °C, (e) 1100 °C, (f) 1150 °C, and (g) 1200 °C.

There are two possible mechanisms responsible for the nucleation of the template BNT grains on the surface of plate-like $BaTiO_3$ grains. These are dissolution-precipitation and spreading. In the dissolution-precipitation mechanism [9], the BNT grains and the plate-like $BaTiO_3$ grains are separated by a liquid phase. The BNT grains dissolve in the liquid phase and precipitate on the surface of the plate-like $BaTiO_3$ grains. The nuclei have the same crystallographic orientation as the plate-like $BaTiO_3$ grains. In the spreading mechanism [6,34], the

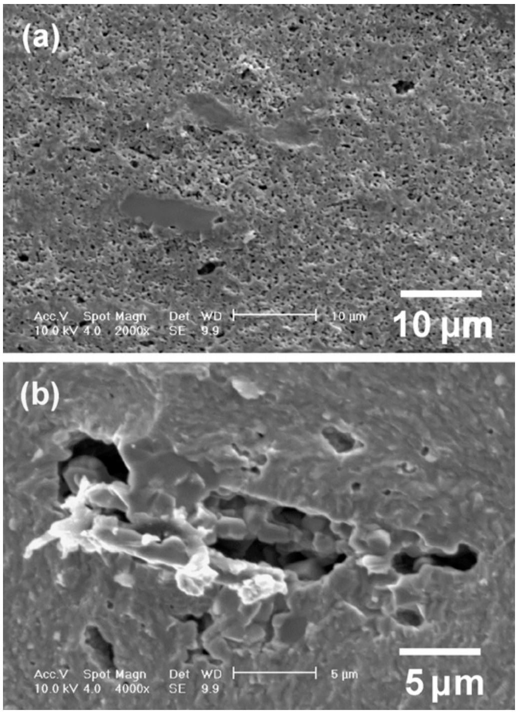

Fig. 12. Microstructures of $BaTiO_3$–(BNT + Bi_2O_3) sintered at (a) 1050 °C and (b) 1100 °C for 2 h.

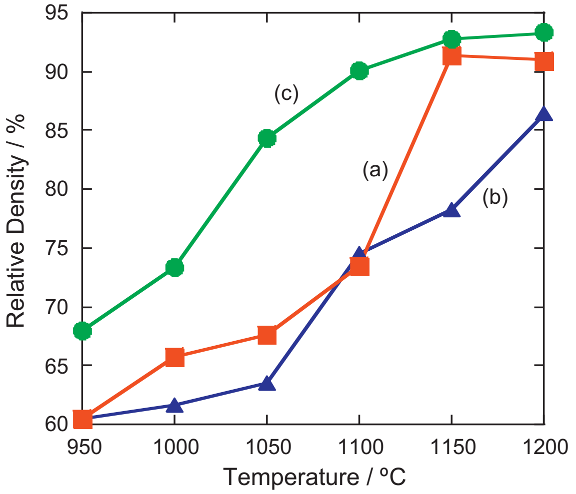

Fig. 13. Relative density of (a) $BaTiO_3$–BNT, (b) $BaTiO_3$–(BNT + Na_2CO_3), and (c) $BaTiO_3$–(BNT + Bi_2O_3) sintered for 2 h.

BNT grains attached to the plate-like $BaTiO_3$ grains form terraces, which have the same crystallographic orientation as the plate-like $BaTiO_3$ grains. The growth of these terraces at the expense of BNT grains results in the formation of template BNT grains. It is not possible to determine which mechanism alone is responsible for the formation of the template BNT grains from the microstructure observation.

Once the surface of the plate-like $BaTiO_3$ grains are covered with the template BNT grains (Fig. 10(a)), the curvature of the surfaces of template BNT grains is almost the same as that of the plate-like $BaTiO_3$ grains and smaller than that of the matrix BNT grains. The difference in the curvature produces the driving force for the growth of the template BNT grains at the expense of the matrix BNT grains. Thus, the template BNT grains can act as templates for texture development even though the plate-like $BaTiO_3$ grains have disappeared. The liquid phase formed by excess Bi_2O_3 does not promote texture development (Fig. 11). Probably, the liquid phase distributes between the matrix BNT grains and promotes their neck growth resulting in densification. Therefore, the formation of template BNT grains is not promoted.

The growth of the template BNT grains is necessary to obtain highly textured materials. It is achieved by heating at high temperatures for long durations. The $BaTiO_3$–(BNT + Na_2CO_3) specimen was heated at 1100 °C for 2 h to form the templated BNT grains and then at 1200 °C for 12 h to grow them. Fig. 14(a) shows the microstructure of this specimen. The microstructure was composed of large grains with a square shape and small irregularly shaped grains. The former grains are formed by the growth of the template BNT grains, and the degree of orientation is 0.46. The angles between the square edges and the surface of the specimen were about 45°, indicating that these grains have a three-dimensional cubic shape and are surrounded by {1 0 0} faces [22]. In general, the faceted surfaces of grains have a low growth rate. In the present case, the cubic grains have faceted surfaces and the growth rate is low. Therefore, further growth cannot be expected by heating them more. Furthermore, prolonged heating increases the size of the matrix grains and reduces the driving force for the growth of the template BNT grains. For example, heating at 1200 °C for 20 h cannot reduce the volume of small grains (Fig. 14(b)). To increase the degree of orientation, the number of the plate-like $BaTiO_3$ grains must be increased by increasing the $BaTiO_3$ content in the formulation or by reducing the thickness of the plate-like $BaTiO_3$ grains.

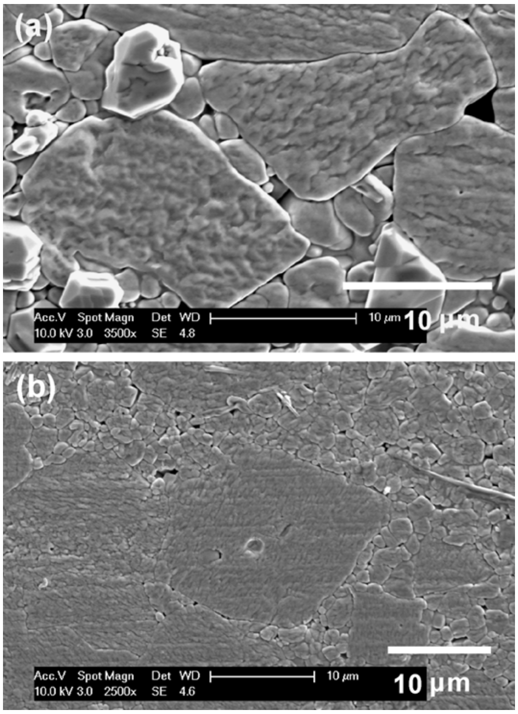

Fig. 14. Microstructures of $BaTiO_3$–(BNT + Na_2CO_3) sintered at 1100 °C for 2 h and then at 1200 °C for (a) 12 h and (b) 20 h.

The dissolution of the plate-like $BaTiO_3$ grains in the BNT matrix creates two problems. One is the formation of large pores as shown in Figs. 10(c) and (d), and the other is the deviation of the composition of the matrix phase. The former problem can be solved by heating at high temperatures for long durations. Fig. 14(b) shows that the central grain has a small circular pore in the grain. This indicates that the volume of the large pores can be reduced by heating at 1200 °C for 20 h. The second problem is related to the overall composition of the sintered compact. The formation of the BNT–$BaTiO_3$ solid solution is inevitable. Fortunately, materials in the BNT–$BaTiO_3$ and BNT–BKT-$BaTiO_3$ solid solutions are expected to have high piezoelectric properties [35]. The plate-like $BaTiO_3$ grains can be used as the Ba source for these solid solutions.

4. Conclusions

The preparation of ⟨1 1 1⟩-textured BNT ceramics was attempted by the TGG method using plate-like $BaTiO_3$ grains with the ⟨1 1 1⟩ direction perpendicular to the plate face. The $BaTiO_3$ grains dissolved in the BNT matrix and disappeared during sintering. Therefore, the textured BNT ceramics could not be obtained. Several different approaches were tried to develop the texture by reducing the dissolution rate. These included the use of plate-like (Sr, Ba)TiO_3 grains as templates and BNT–$BaTiO_3$ and BNT–BKT solid solutions as the matrix, as well as the formation of a liquid phase by adding excess Na_2CO_3 and Bi_2O_3. The approach that was successful was the addition of excess Na_2CO_3. Excess Na_2CO_3 formed a liquid phase and promoted the formation of BNT shells around the plate-like $BaTiO_3$ grains, prior to the dissolution of $BaTiO_3$ grains. The BNT shells had the same crystallographic orientation as the plate-like $BaTiO_3$ grains and acted as templates for the texture development.

References

[1] T. Kimura, Application of texture engineering to piezoelectric ceramics – a review, J. Ceram. Soc. Jpn. 114 (2006) 15–25.

[2] G.L. Messing, S. Trolier-McKinstry, E.M. Sabolsky, C. Duran, S. Kwon, B. Brahmaroutu, P. Park, H. Yilmaz, P.W. Rehrig, K.B. Eitel, E. Suvaci, M. Seabaugh, K.S. Oh, Templated grain growth of textured piezoelectric ceramics, Crit. Rev. Solid State Mater. Sci. 29 (2004) 45–96.

[3] M.M. Seabaugh, G.L. Messing, M.D. Vaudin, Texture development and microstructure evolution in liquid-phase-sintered α-alumina ceramics prepared by templated grain growth, J. Am. Ceram. Soc. 83 (2000) 3109–3116.

[4] E. Suvaci, G.L. Messing, Critical factors in the templated grain growth of textured reaction-bonded alumina, J. Am. Ceram. Soc. 83 (2000) 2041–2048.

[5] T. Kimura, Y. Yoshida, Origin of texture development in barium bismuth titanate made by templated grain growth method, J. Am. Ceram. Soc. 89 (2006) 869–874.

[6] T. Shoji, K. Fuse, T. Kimura, Mechanism of texture development in $Bi_{0.5}(Na, K)_{0.5}TiO_3$ made by templated grain growth process, J. Am. Ceram. Soc. 92 (2009) S140–S145.

[7] T. Tani, T. Kimura, Reactive-templated grain growth processing for lead-free piezoelectric ceramics, Adv. Appl. Ceram. 105 (2006) 55–63.

[8] T. Tani, Texture engineering of electronic ceramics by the reactive-templated grain growth method, J. Ceram. Soc. Jpn. 114 (2006) 363–370.

[9] S. Trolier-McKinstry, E. Sabolsky, S. Kwon, C. Duran, T. Yoshimura, J.-H. Park, Z. Zhang, G.L. Messing, Oriented films and ceramics of relaxor ferroelectric – $PbTiO_3$ solid solutions, in: N. Setter (Ed.), Piezoelectric Materials in Devices, Ceramic Laboratory, EPFL, Lausanne, 2002, pp. 497–518.

[10] H. Yilmaz, G.L. Messing, S. Trolier-McKinstry, (Reactive) Templated grain growth of textured sodium bismuth titanate ($Na_{1/2}Bi_{1/2}TiO_3$–$BaTiO_3$) ceramics. I. Processing, J. Electroceram. 11 (2003) 207–215.

[11] K. Watari, B. Brahmaroutu, G.L. Messing, S. Trolier-McKinstry, Epitaxial growth of anisotropically shaped, single-crystal particles of cubic $SrTiO_3$, J. Mater. Res. 15 (2000) 846–849.

[12] Y. Saito, H. Takao, T. Tani, T. Nonoyama, K. Takatori, T. Homma, T. Nagaya, M. Nakamura, Lead-free piezoceramics, Nature 432 (2004) 84–87.

[13] D. Liu, Y. Yan, H. Zhou, Synthesis of micron-scale platelet $BaTiO_3$, J. Am. Ceram. Soc. 90 (2007) 1323–1326.

[14] S.F. Poterala, Y. Chang, T. Clark, R.J. Meyer, G.L. Messing Jr., Mechanistic interpretation of the Aurivillius to perovskite topochemical microcrystal conversion process, Chem. Mater. 22 (2010) 2061–2068.

[15] Y. Saito, H. Takao, Synthesis of platelike {1 0 0} $SrTiO_3$ particles by topochemical microcrystal conversion and fabrication of grain-oriented ceramics, Jpn. J. Appl. Phys. 45 (2006) 7377–7381.

[16] J.T. Zeng, K.W. Kwok, W.K. Tam, H.Y. Tian, X.P. Jiang, H.L.W. Chan, Plate-like $Na_{0.5}Bi_{0.5}TiO_3$ template synthesized by a topochemical method, J. Am. Ceram. Soc. 89 (2006) 3850–3853.

[17] W. Zhao, H. Zhou, Y. Yan, D. Liu, Topochemical synthesis of plate-like $Na_{0.5}Bi_{0.5}TiO_3$ from Aurivillius precursor, J. Am. Ceram. Soc. 91 (2008) 1322–1325.

[18] Y. Saito, H. Takao, K. Wada, Synthesis of platelike $CaTiO_3$ particles by a topochemical microcrystal conversion method and fabrication of textured microwave dielectric ceramics, Ceram. Int. 34 (2008) 745–751.

[19] S. Wada, S. Suzuki, T. Noma, T. Suzuki, M. Osada, M. Kakihana, S.-E. Park, L.E. Cross, T.R. Shrout, Enhanced piezoelectric property of barium titanate single crystals with engineered domain configuration, Jpn. J. Appl. Phys. Part 1 38 (1999) 5505–5511.

[20] T. Sato, T. Kimura, Preparation of $\langle 1\,1\,1 \rangle$-textured $BaTiO_3$ ceramics by templated grain growth method using novel template particles, Ceram. Int. 34 (2008) 757–760.

[21] S. Wada, K. Takeda, T. Muraishi, H. Kakemoto, T. Tsurumi, T. Kimura, Preparation of [1 1 0] grain oriented barium titanate ceramics by templated grain growth method and their piezoelectric properties, Jpn. J. Appl. Phys. 46 (2007) 7039–7043.

[22] T. Motohashi, T. Kimura, Formation of homo-template grains in $Bi_{0.5}Na_{0.5}TiO_3$ prepared by reactive-templated grain growth process, J. Am. Ceram. Soc. 91 (2008) 3889–3895.

[23] T. Kimrua, E. Fukuchi, T. Tani, Fabrication of textured bismuth sodium titanate using excess bismuth oxide, Jpn. J. Appl. Phys. 44 (2005) 8055–8061.

[24] T. Kimura, Y. Miura, K. Fuse, Texture development in barium titanate and PMN-PT using hexabarium 17-titanate heterotemplates, Int. J. Appl. Ceram. Technol. 2 (2005) 15–23.

[25] F.K. Lotgering, Topotactical reactions with ferrimagnetic oxides having hexagonal crystal structures. I, J. Inorg. Nucl. Chem. 9 (1959) 113–123.

[26] K.W. Kirby, B.A. Wechsler, Phase relations in the barium titanate–titanium oxide system, J. Am. Ceram. Soc. 74 (1991) 1841–1847.

[27] Y. Abe, T. Kimura, Factors determining grain orientation in bismuth sodium potassium titanate–lead zirconate titanate solid solutions made by reactive templated grain growth method, J. Am. Ceram. Soc. 85 (2002) 1114–1120.

[28] K. Kato, T. Kimura, Preparation of textured $Bi_{0.5}(Na, K)_{0.5}TiO_3$–$BiFeO_3$ solid solutions by reactive-templated grain growth process, J. Korean Ceram. Soc. 43 (2006) 693–699.

[29] G.O. Jones, P.A. Thomas, Investigation of the structure and phase transformations in the novel A-site substituted distorted perovskite compound $Na_{0.5}Bi_{0.5}TiO_3$, Acta Crystallogr. Sect. B B58 (2002) 168–178.

[30] T. Takenaka, K. Maruyama, K. Sakata, $(Bi_{1/2}Na_{1/2})TiO_3$–$BaTiO_3$ system for lead-free piezoelectric ceramics, Jpn. J. Appl. Phys. Part 1 30 (1991) 2236–2322.

[31] E. Fukuchi, T. Kimura, T. Tani, T. Takeuchi, Y. Saito, Effect of potassium concentration on the grain orientation in bismuth sodium potassium titanate, J. Am. Ceram. Soc. 85 (2002) 1461–1466.

[32] M.-G. Lee, S.-Y. Chung, S.-J.L. Kang, Boundary faceting-dependent densification in a $BaTiO_3$ model system, Acta Mater. 59 (2011) 692–698.

[33] K.-S. Moon, S.-J.L. Kang, Coarsening behavior of round-edged cubic grains in the $Na_{1/2}Bi_{1/2}TiO_3$–$BaTiO_3$ system, J. Am. Ceram. Soc. 91 (2008) 3191–3196.

[34] D. Ijuu, T. Kimura, T. Yamada, H. Funakubo, Preparation and characteristics of $Bi_{0.5}Na_{0.5}TiO_3$ single-crystalline films by a solid-state process, J. Am. Ceram. Soc. 94 (2011) 3291–3295.

[35] S.O. Leontsev, R.E. Eitel, Progress in engineering high strain lead-free piezoelectric ceramics, Sci. Technol. Adv. Mater. 11 (2010) 044302.